

A methodology to evaluate fluid-dynamic forces on immersed bodies in 3D fluid flow problems

André S. Müller¹, Eduardo M. B. Campelo¹, Henrique C. Gomes¹

¹*Dept. of Structural and Geotechnical Engineering, Polytechnic School, University of São Paulo
Av. Prof. Almeida Prado, Lane 3, 380, 05508-010, São Paulo/SP, Brazil
andre.muller@ifma.edu.br, campello@usp.br, henrique.campelo@usp.br*

Abstract. This work presents first results on a methodology to evaluate fluid-dynamic forces on immersed bodies in three-dimensional fluid flows resolved through the finite element method (FEM). A classical Eulerian approach is followed to describe the fluid (assumed incompressible through the Navier-Stokes equations). The fluid-body interface is treated through Nitsche's method, which is an immersed boundary technique with which we consistently impose the Dirichlet boundary conditions in a weak form. In order to assess the accuracy and efficiency of the developed scheme, a numerical simulation of a 3D benchmark stationary flow of an incompressible fluid is performed. This work refers to an intermediate stage of a doctoral research that aims to model fluid flows with immersed particles with consistent fluid-particle interaction and particle-to-particle contacts, as observed in many particle-laden fluid applications.

Keywords: fluid-dynamic forces, immersed boundary techniques, Nitsche's method, finite element method.

1 Introduction

In the fluid-body interaction realm, if we restrict ourselves to the way how the numerical method handles the interface between the fluid and the body (solid) phases, the most common numerical approaches available may be categorized into two major groups. The first one is commonly referred to as the coincident boundary methods, being those in which the computational grid or mesh of the fluid ends exactly where that of the body begins (see e.g. Donea et al. [1]). The second one are the so-called immersed boundary methods, in which the fluid and the body grids are totally independent from each other, and overlapped (see Benk, Ulbrich and Mehl [2]).

This work follows the immersed boundary approach and presents a methodology to compute the fluid-dynamic forces on immersed bodies in three-dimensional FEM simulations of incompressible fluid flows governed by the Navier-Stokes equations. We resort to the Nitsche's method (see Nitsche [3]) to handle the (immersed) fluid-body interface. Among other advantages, it does not increase the system's degrees of freedom and has a rather straightforward implementation. The fluid problem is treated through an Eulerian description, which avoids re-meshing or mesh adaptation throughout the simulations. Here, only the stationary version of the problem is presented (the transient version is currently under development by the authors, using standard Newmark time-integration, and shall appear soon). For the FEM discretization, a mixed finite element formulation within a standard Galerkin framework is used, with Taylor-Hood tetrahedral elements that fully satisfy the LBB-condition (see e.g. Wieners [4] and Bruman and Fernández [5]). A consistent Newton-Raphson procedure is implemented for solving the system's equations. Numerical instability that may potentially arise from convective-dominated problems is circumvented here by considering only low to moderate Reynolds numbers (we note that we handle such instabilities in our code through a SUPG approach, but prefer not to introduce this additional complexity here as to keep the focus of the work on the methodology for computation of the fluid-dynamic forces). Immersed boundary methods combined with fixed fluid grids have been gaining attention in recent years in the context of embedded interfaces modeled by the XFEM (see Dolbow and Harari [6]), also with imposition of constraints along non-matching surface grids (Bazilevs and Hughes [7]).

This work reports only partial results from a broader research, in which we are developing a numerical framework to deal with 3D fluid-particle interaction problems in particle-laden fluid flows.

2 Finite element formulation for the fluid

Considering an incompressible viscous fluid governed by Navier-Stokes equations for steady-state problems, we have

$$(\nabla \mathbf{u})\mathbf{u} = \operatorname{div} \mathbf{T} + \rho \mathbf{b} \quad \text{in } \Omega, \quad (1)$$

$$\operatorname{div} \mathbf{u} = 0 \quad \text{in } \Omega, \quad (2)$$

where (1) is the well-known conservation of linear momentum of a material point of the fluid and (2) follows from the mass conservation principle. Above, ρ , \mathbf{u} , \mathbf{T} and \mathbf{b} are the fluid's density, velocity field, Cauchy stress field and volumetric force per unit mass, respectively, with Ω as the problem domain. For an Eulerian description and a Newtonian constitutive law for the fluid, the following system arises from (1) and (2):

$$\begin{aligned} (\nabla \mathbf{u})\mathbf{u} - 2\nu \operatorname{div}(\nabla^s \mathbf{u}) + \nabla p &= \mathbf{b} \quad \text{in } \Omega, \\ \operatorname{div} \mathbf{u} &= 0 \quad \text{in } \Omega, \\ \mathbf{u} &= \bar{\mathbf{u}} \quad \text{in } \Gamma_u, \\ \mathbf{T}\mathbf{n} &= \bar{\mathbf{t}} \quad \text{in } \Gamma_t, \end{aligned} \quad (3)$$

where ν is the fluid's kinematic viscosity, $\nabla^s \mathbf{u}$ is the (symmetric) strain rate tensor and p the fluid's kinematic pressure. Vector \mathbf{n} stands for the unit outward normal to the boundary Γ , and $\bar{\mathbf{u}}$ and $\bar{\mathbf{t}}$ are the prescribed traction and velocity vectors, respectively, on the portions Γ_u and Γ_t of Γ . The third and fourth expressions of (3) represent the boundary conditions of Dirichlet (essential) and Neumann (natural) types, respectively.

The weak form of (3) reads

$$c(\mathbf{u}; \mathbf{w}, \mathbf{u})_\Omega + a(\mathbf{w}, \mathbf{u})_\Omega - (\operatorname{div} \mathbf{w}, p)_\Omega + (q, \operatorname{div} \mathbf{u})_\Omega - (\mathbf{w}, \bar{\mathbf{t}})_{\Gamma_t} = (\mathbf{w}, \mathbf{b})_\Omega \quad \forall \mathbf{w}, q, \quad (4)$$

where \mathbf{w} and q are arbitrary test functions for the velocity and pressure fields, respectively. The trilinear and bilinear forms of the convective and viscous terms above are

$$c(\mathbf{u}; \mathbf{w}, \mathbf{u})_\Omega = \int_\Omega \mathbf{w} \cdot (\nabla \mathbf{u}) \mathbf{u} d\Omega \quad \text{and} \quad a(\mathbf{w}, \mathbf{u})_\Omega = \int_\Omega \nabla \mathbf{w} : \nu \nabla \mathbf{u} d\Omega. \quad (5)$$

2.1 Spatial discretization

A standard mixed finite element scheme is applied for spatial discretization, where the velocity and pressure fields are the primitive variables of the problem and the fluid's domain is discretized with Taylor-Hood tetrahedral elements (see Taylor and Hood [8]). Such elements use quadratic shape functions for the velocity field and linear shape functions for the pressure field, therewith overcoming numerical instabilities (they fulfill the LBB compatibility condition). Accordingly, the finite element approximation can be written as

$$\begin{aligned} \mathbf{u} &\approx \mathbf{N}_u \mathbf{u}_e \quad \text{and} \quad p \approx \mathbf{N}_p \mathbf{p}_e, \\ \mathbf{w} &\approx \mathbf{N}_u \mathbf{w}_e \quad \text{and} \quad q \approx \mathbf{N}_p \mathbf{q}_e, \end{aligned} \quad (6)$$

where \mathbf{N}_u and \mathbf{N}_p are matrices that contain the element's shape functions of the velocity and pressure fields, respectively, and \mathbf{u}_e and \mathbf{p}_e are the vectors that collect the element's nodal degrees of freedom. Inserting eq. (6) into the weak form (4), and performing some algebra, we arrive at the discrete weak form of the fluid problem, which in matrix form is given by

$$\begin{cases} \mathbf{C}(\mathbf{u})\mathbf{u} + \mathbf{K}\mathbf{u} + \mathbf{G}\mathbf{p} = \mathbf{f} \\ \mathbf{G}^T \mathbf{u} = \mathbf{0} \end{cases}, \quad (7)$$

where \mathbf{C} , \mathbf{K} , \mathbf{G} and \mathbf{G}^T are the convective, viscous, gradient operator and divergent operator matrices, respectively. Still in (7), \mathbf{f} is the vector that contains the field forces and boundary conditions. The system of equations (7) is non-linear due to the convective term, and its solution is achieved using a consistent Newton-Raphson scheme for which full quadratic convergence is ensured. For more details about its numerical derivation and implementation, the interested reader is referred to Müller et al. [9] (the two-dimensional version may be found

in Gomes and Pimenta [10]).

3 Imposing the interface condition

The main idea of this work is to use the embedded interface concept in order to compute the fluid flow variables at the fluid-body interface from an Eulerian fixed mesh. To do so, we resort to the Nitsche's method to enforce the interface constraints (Dirichlet boundary conditions) in a weak sense, for treating the mechanical interactions of overlapping meshes, as depicted in Figure 1. One of the greatest advantages of this method is that it does not add new degrees of freedom to the system.

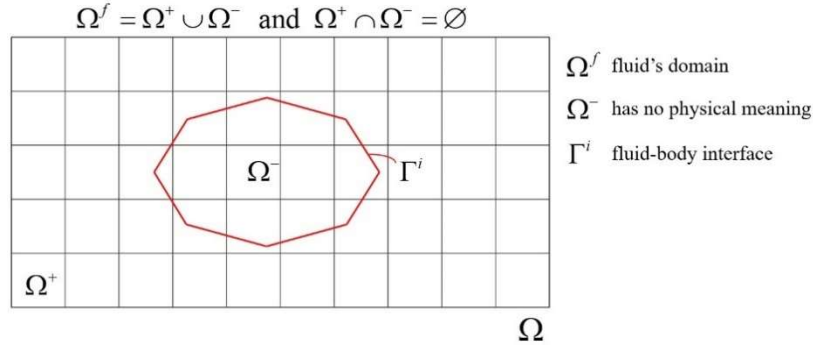


Figure 1. Immersed solid in a fluid and the embedded fluid-body interface. The interface is discretized into interface elements as to enable the computations. Superscript i stands for the body's number.

By applying Nitsche's method in (4), after some algebra the weak form turns into

$$\begin{aligned}
 & c(\mathbf{u}; \mathbf{w}, \mathbf{u})_{\Omega} + a(\mathbf{w}, \mathbf{u})_{\Omega} - (\operatorname{div} \mathbf{w}, p)_{\Omega} + (q, \operatorname{div} \mathbf{u})_{\Omega} - \nu \langle \partial_n \mathbf{u}, \mathbf{w} \rangle_{\Gamma^i} \\
 & - \nu \langle \partial_n \mathbf{w}, \mathbf{u} \rangle_{\Gamma^i} + \langle p \mathbf{n}, \mathbf{w} \rangle_{\Gamma^i} - \langle q \mathbf{n}, \mathbf{u} \rangle_{\Gamma^i} + \nu \frac{\alpha_1}{h} \langle \mathbf{u}, \mathbf{w} \rangle_{\Gamma^i} + \frac{\alpha_2}{h} \langle \mathbf{u} \cdot \mathbf{n}, \mathbf{w} \cdot \mathbf{n} \rangle_{\Gamma^i} \\
 & = (\mathbf{w}, \bar{\mathbf{t}})_{\Gamma^i} + (\mathbf{w}, \mathbf{b})_{\Omega} - \nu \langle \partial_n \mathbf{w}, \bar{\mathbf{u}} \rangle_{\Gamma^i} - \langle q \mathbf{n}, \bar{\mathbf{u}} \rangle_{\Gamma^i} + \nu \frac{\alpha_1}{h} \langle \bar{\mathbf{u}}, \mathbf{w} \rangle_{\Gamma^i} + \frac{\alpha_2}{h} \langle \bar{\mathbf{u}} \cdot \mathbf{n}, \mathbf{w} \cdot \mathbf{n} \rangle_{\Gamma^i} \quad \forall \mathbf{w}, q,
 \end{aligned} \tag{8}$$

where h denotes the local mesh size on the boundary Γ^i (or immersed interface) of body i , $\partial_n(\cdot)$ is the normal derivative of (\cdot) , and α_1 and α_2 are penalty coefficients. The discrete weak form of eq. (8) in matrix form reads

$$\begin{cases} \mathbf{C}(\mathbf{u}) \mathbf{u} + \mathbf{K}^* \mathbf{u} + \mathbf{G}^* \mathbf{p} = \mathbf{f} + \mathbf{H} \bar{\mathbf{u}} \\ \mathbf{G}^{\mathbf{T}*} \mathbf{u} = \mathbf{0} \end{cases}, \tag{9}$$

where

$$\begin{aligned}
 \mathbf{K}^* &= \mathbf{K} + \mathbf{B} + \mathbf{B}^{\mathbf{T}} + \mathbf{E} + \mathbf{F}, \quad \mathbf{G}^* = \mathbf{G}_e + \mathbf{D}, \quad \mathbf{G}^{\mathbf{T}*} = \mathbf{G}_e^{\mathbf{T}} + \mathbf{D}^{\mathbf{T}}, \quad \text{and } \mathbf{H} = \mathbf{B}^{\mathbf{T}} + \mathbf{E} + \mathbf{F}, \\
 \mathbf{B} &= \sum_e \mathbf{A}_e^{\mathbf{T}} \int_{\Gamma^i} -\nu \mathbf{N}_u^{\mathbf{T}} [\mathbf{N}_{u,j} (\mathbf{e}_j^{\mathbf{T}} \mathbf{n})] d\Gamma^i \mathbf{A}_e, \quad \mathbf{D} = \sum_e \mathbf{A}_e^{\mathbf{T}} \int_{\Gamma^i} [\mathbf{n}^{\mathbf{T}} \mathbf{N}_u]^{\mathbf{T}} \mathbf{N}_p d\Gamma^i \mathbf{A}_e, \\
 \mathbf{E} &= \sum_e \mathbf{A}_e^{\mathbf{T}} \left(\nu \frac{\alpha_1}{h} \right) \int_{\Gamma^i} \mathbf{N}_u^{\mathbf{T}} \mathbf{N}_u d\Gamma^i \mathbf{A}_e \quad \text{and} \quad \mathbf{F} = \sum_e \mathbf{A}_e^{\mathbf{T}} \left(\frac{\alpha_2}{h} \right) \int_{\Gamma^i} [\mathbf{n}^{\mathbf{T}} \mathbf{N}_u]^{\mathbf{T}} [\mathbf{n}^{\mathbf{T}} \mathbf{N}_u] d\Gamma^i \mathbf{A}_e,
 \end{aligned} \tag{10}$$

in which \mathbf{A}_e is the assembling matrix relative to the interface elements of Γ^i . The interested reader is referred to Bank, Ulbrich and Mehl [2] for more details on the Nitsche's method applied to the Navier-Stokes equations.

3.1 Evaluating the fluid-dynamic forces at the immersed interface

The immersed interfaces are the regions where the fluid-dynamic forces between the fluid and the immersed body take place. The usual way to evaluate the resultant of these forces, herein designated by \mathbf{f}_{Γ^i} , are through

$$\mathbf{f}_{\Gamma^i} = \oint_{\Gamma^i} \mathbf{T}\mathbf{n} d\Gamma^i. \quad (11)$$

However, the boundary Γ^i of each immersed body is discretized into k Lagrangian elements (see Figure 2(b)), such that the fluid-dynamic force at each element can be evaluated by

$$\mathbf{f}_{\Gamma_k^i} = \oint_{\Gamma_k^i} \mathbf{T}\mathbf{n} d\Gamma_k^i \text{ and,} \quad (12)$$

where Γ_k^i is the boundary of the element k belonging to the immersed body i . The moment of each element k , in turn, with respect to the barycenter of the body i , may be obtained by

$$\mathbf{m}_{\Gamma_k^i} = \mathbf{r}_k^i \times \mathbf{f}_{\Gamma_k^i}, \quad (13)$$

where \mathbf{r}_k^i is the vector that connects the barycenter of the body i to the point C_k^i (this is the center of each element k used to discretize the immersed body i , see Figure 2(b)) on its boundary where traction $\mathbf{T}\mathbf{n}$ acts. It is known that the use of penalty-based methods, such as Nitsche's, by weakly imposing Dirichlet boundary conditions on the fluid-body interface, can cause disturbances in the pressure and velocity fields in the vicinity of Γ^i . As a consequence, the above computations of $\mathbf{f}_{\Gamma_k^i}$ and $\mathbf{m}_{\Gamma_k^i}$ can be severely affected. Here we propose a methodology to overcome this problem. It is inspired by the work of Chadil et al. [11]. Accordingly, $\mathbf{f}_{\Gamma_k^i}$ is obtained by a linear extrapolation of the pressure and the velocity gradient values in the region nearest to Γ_k^i where the perturbation of the extrapolated values (in PE1 and PE2, see Figure 2(b)) is minimized. Such values are obtained using the interpolation function of the element these points belong to. According to Chadil, this region has the size of the cut element size (Δx), as depicted in Figure 2.

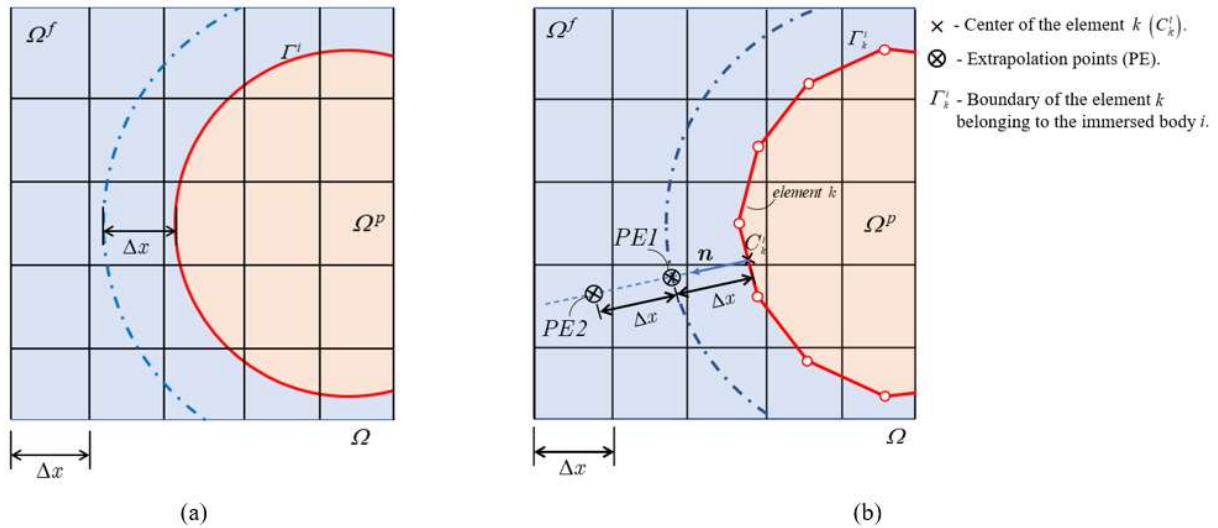


Figure 2. (a) Vicinity of interface Γ^i where the values of the pressure field can be disturbed; (b) Scheme for obtaining the points at which pressure and velocity gradient values are extrapolated.

With the extrapolated values in C_k^i , the fluid-dynamic forces at Γ_k^i can be evaluated by (11) and (13). The equation (14) shows how the resultant force and the respective resultant moment on each immersed body can be obtained.

$$\mathbf{f}_R = \sum_{i=1}^{nel\Gamma} \mathbf{f}_{\Gamma_k^i} \text{ and } \mathbf{m}_R = \sum_{i=1}^{nel\Gamma} \mathbf{m}_{\Gamma_k^i}, \quad (14)$$

where $nel\Gamma$ is the number of interface elements associated with Γ^i .

4 Numerical example

4.1 3D Laminar flow around a cylinder

This example consists of a stationary three-dimensional laminar flow around a cylinder with circular cross-section within a narrow channel, which is a classical benchmark in the CFD community (see e.g. Schäfer and Turek [12], Bayraktar, Mierka and Turek [13], Turek and Schäfer [14]). The fluid is governed by the Navier-Stokes equation. The geometry and the boundary conditions are illustrated in Figure 3.

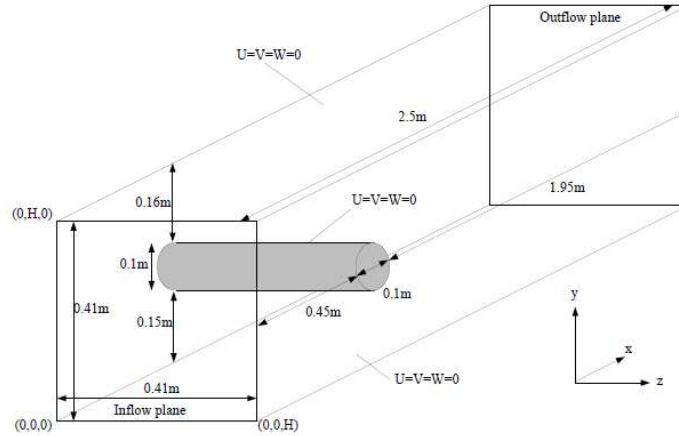


Figure 3. Geometry and boundary conditions for 3D laminar flow around a cylinder with circular cross-section (figure from Schäfer and Turek [12]).

The fluid velocity profile at the inflow section of the channel is

$$U(0, y, z) = \frac{16U_m yz(H-y)(H-z)}{H^4}, \quad V = W = 0 \quad (15)$$

where $U_m = 0.45$ m/s and $H = 0.41$ m, from which the Reynolds number is $Re = 20$. The kinematic viscosity is $\nu = 10^{-3}$ m²/s, and the fluid density is $\rho = 1.0$ kg/m³. Notation for the velocity components is $(u_1, u_2, u_3) = (U, V, W)$ and the boundary condition at the outflow plane is zero traction. The penalty coefficients used are $\alpha_1 = \alpha_2 = 10^7$. The convergence tolerance within the Newton-Raphson iterations is $TOL = 10^{-6}$. Figure 4 shows the fluid FEM mesh (left) and the cylinder's interface mesh (right) used herein.

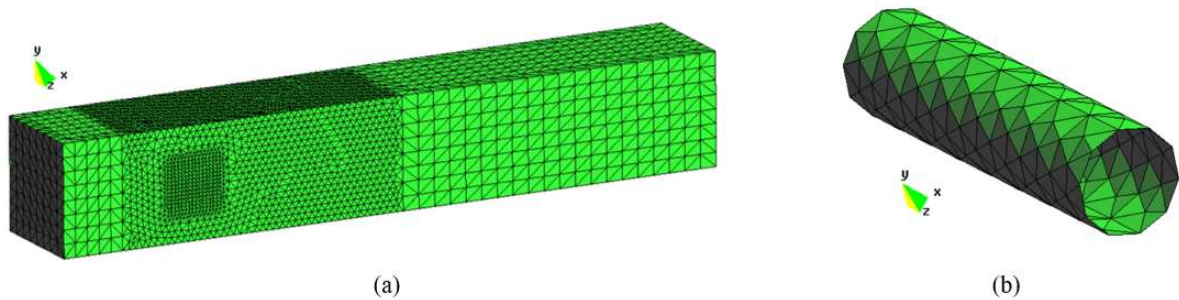


Figure 4. (a) Fluid FEM mesh: 158082 tetrahedral elements and 220324 nodes; (b) Interface (Lagrangian) mesh: 320 triangular elements and 170 nodes.

Figure 5 depicts the results in terms of the velocity and pressure fields obtained. The resulting drag coefficient on the cylinder is summarized in Table 1. As we can see, the drag coefficient value is within the reference interval

shown in Schäfer and Turek [12]. It is important to remark that the refinement of the mesh around the interface Γ^i and the correct choice of penalty parameters have a rather significant importance in the accuracy of the result. Details on this issue are being investigated and will be subject of a forthcoming paper (in preparation) in a journal.

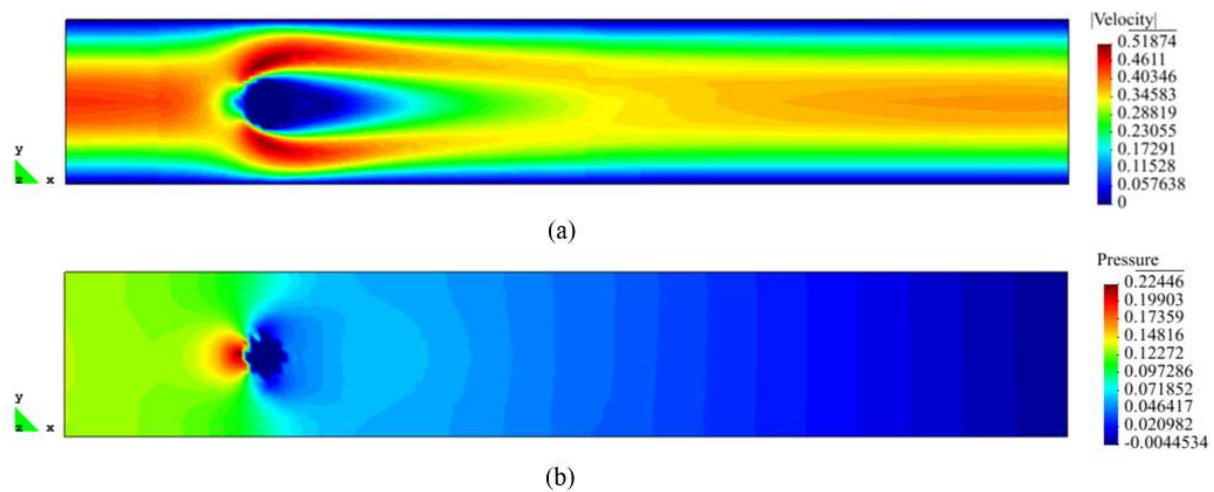


Figure 5. Velocity and pressure fields.

Table 1. C_D coefficient.

		C_D
Present work		6,0800
[Schäfer and Turek]	Upper bound	6,2500
	Lower bound	6,0500

5 Conclusions

This work presented a summary of a methodology to compute the fluid-dynamic forces on an immersed body within a fluid. A mixed finite element formulation of an incompressible fluid flow governed by stationary Navier-Stokes equation was used, along with Nitsche's method to enforce the Dirichlet boundary conditions in a weak form at the interface. We showed our first results for 3D simulations using such methodology. Its extension to other shapes of immersed bodies (especially spherical, in which we have interest for enabling the simulation of particle-laden fluids) and to transient problems is currently under work. We find the present results very promising. A detailed report of this methodology and its application to other (including transient) problems, including fixed and moving immersed bodies, are the subject of a paper that will be published in a journal in the near future.

Acknowledgements. First author acknowledges support by the Federal Institute of Maranhão, Brazil, and by the Department of Civil Construction. Also acknowledges scholarship funding from FAPEMA (Fundação de Amparo à Pesquisa e ao Desenvolvimento Científico e Tecnológico do Maranhão) under the grant BD-02045/19. Second author acknowledges support by CNPq (Conselho Nacional de Desenvolvimento Científico e Tecnológico), Brazil, under the grants 307368/2018-1 and 313046/2021-2.

Authorship statement. The authors hereby confirm that they are the sole liable persons responsible for the authorship of this work, and that all material that has been herein included as part of the present paper is either the property (and authorship) of the authors, or has the permission of the owners to be included here.

References

- [1] J. Donea, A. Huerta, J.-P. Ponthot and A. Rodríguez-Ferran, Arbitrary Lagrangian-Eulerian Methods. In: Stein E, De Borst R, Hughes TJR (eds) Encyclopedia of computational mechanics, New York: Wiley, 2004.
- [2] J. Benk, M. Ulbrich and M. Mehl, "The Nitsche method of the Navier-Stokes equations for immersed and moving boundaries," in *Seventh International Conference on Computational Fluid Dynamics*, Big Island, Hawaii, 2012.
- [3] J. Nitsche, "Über ein Variationsprinzip zur Lösung von Dirichlet-problemen bei Verwendung von Teilräumen, die keinen Randbedingungen unterworfen sind," *Abh. Math. Sem. Univ. Hamburg*, pp. 9-15, 1971.
- [4] C. Wieners, Taylor-Hood elements in 3D. In: Wendland, W.; Efendiev, M. (eds) Analysis and simulation of multifield problems. Lecture Notes in Applied and Computational Mechanics, Berlin: Springer, 2003.
- [5] E. Burman and M. A. Fernández, "Stabilized finite element schemes for incompressible flow using velocity/pressure spaces satisfying the LBB-condition," in *Proceedings of the WCCM VI*, Beijing, 2004.
- [6] J. Harari and I. Dolbow, "An efficient finite element method for embedded interface problems.," *International Journal for Numerical Method in Engineering*, pp. 229-252, 2009.
- [7] Y. Hughes and T. Bazilevs, "Nurbs-based isogeometric analysis for the computation of flows about rotating components," *Computational Mechanics*, pp. 143-150, 2008.
- [8] C. Hood and P. Taylor, "A numerical solution of the Navier-Stokes equations using the finite element technique," *Computers & Fluids*, pp. 73-100, 1973.
- [9] A. S. Müller, E. M. B. Campello, H. C. Gomes and G. C. Buscaglia, "A numerical method for the three-dimensional simulation of particle-laden fluid flows (in preparation)," *Computer Methods in Applied Mechanics and Engineering*, vol. n/a, p. n/a, 2023.
- [10] H. C. Gomes and P. M. Pimenta, "Embedded interface with discontinuous Lagrange Multipliers for fluid-structure interaction analysis," *International Journal for Computational Methods in Engineering Science and Mechanics*, pp. 1177-1226, 2015.
- [11] M. A. Chadil, S. Vincent e J. L. Estivalèzes, "Accurate estimate of drag forces using particle-resolved direct numerical simulations," *Acta Mech*, 2019.
- [12] M. Schäfer e S. Turek, "Benchmark computations of laminar flow around a cylinder," *Numer. Fluid Mech.*, pp. 547-566, 1996.
- [13] E. Bayraktar, O. Mierka e S. Turek, "Benchmark computations of 3D laminar flow around a cylinder with CFX, OpenFOAM and FeatFlow," *International Journal of Comp. Science and Eng.*, pp. 253-266, 2012.
- [14] S. Turek e M. Schäfer, "Recent benchmark computations of laminar flow around a cylinder," *Proceedings of the 3rd World Conference in Applied Computational Fluid Mechanics*, 1996.